Structural Engineering and Mechanics, *Vol. 55, No. 1 (2015) 65-78*
DOI: http://dx.doi.org/10.12989/sem.2015.55.1.065

Finite element analysis in static and dynamic behaviors of dental prosthesis

N. Djebbar*, B. Serier[a] and B. Bachir Bouiadjra[b]

Department of Mechanical Engineering, University of Sidi Bel Abbes, BP 89, Cité Ben M'hidi, Sidi Bel Abbes 22000, Algeria

(Received November 27, 2014, Revised February 27, 2015, Accepted April 3, 2015)

Abstract. In recent years, implants have gained growing importance in all areas of medicine. The success of the treatment depends on many factors affecting the bone–implant, implant–abutment and abutment–prosthesis interfaces. In this paper, static and dynamic behaviors of the dental prosthesis are investigated. Three-dimensional finite element models of dental prosthesis were constructed. Dynamic loads in 5 sec applied on occlusal surface. Therefore, FEA was selected for use in this study to examine the effect of the static and dynamic loads on the stress distribution for an implant-supported fixed partial denture and supporting bone tissue.

Keywords: static and dynamic loading; finite element analysis; dental prosthesis

1. Introduction

Single-tooth dental implants provide an excellent prosthetic solution for the partially edentulous patient by Zarb and Schmitt (1990). Stresses fields around osseointegrated dental implants are affected by a number of biomechanical factors, including the type of loading, material properties of the implant and the prosthesis, implant geometry, surface structure, quality and quantity of the surrounding bone, and the nature of the bone–implant interface (Koca *et al.* 2005, Brunski *et al.* 1997). However, in several challenging clinical situations, it is difficult to achieve adequate fixation (osseointegration) between the implant and bone. In difficult cases like immediate loading, aesthetic areas or reduced bone placement is challenging by Zinser *et al.* (2004). Many clinical studies have documented the long-term success of dental implants with reported success rates of up to 99%, single tooth replacement has gained more and more importance in dental practice (Dittmer *et al.* 2011). The success or failure of an implant is determined by the manner that the stresses at the bone- implant interface transfer to the surrounding bones (Van Osterwyck *et al.* 1998, Geng *et al.* 2001). The dynamic, static and fatigue behaviours of the implant were studied by Kayabasi *et al.* (2006). Dynamic loads were applied during five minutes to occlusive surface. For the fatigue analysis of the implant, they used the

*Corresponding author, Ph.D., E-mail: djebbarnour@yahoo.fr
[a]Professor, E-mail: serielem@yahoo.fr
[b]Professor, E-mail: bachirbou@yahoo.fr

Copyright © 2015 Techno-Press, Ltd.
http://www.techno-press.org/?journal=sem&subpage=8 ISSN: 1225-4568 (Print), 1598-6217 (Online)

formula of Goodman, Soderberg and Gerber. Rodrigo *et al.* (2011) studied the effect of reinforcements and the space available for their placement on the dynamic and static loading capacity of a simulated implant- supported overdenture model. Scott *et al.* (2001) calculated the fatigue life of UCLA-style abutment screws in wide-diameter versus conventionally sized dental implant restorations. In this study, Ao *et al*. (2010) used a finite element method to evaluate the maximum Von Mises stresses in jaw Bones of immediately loaded implant with different thread heights and widths, and the maximum Displacements in implant-abutment complex. The implant thread height ranged from 0.20 to 0.60 mm, and the thread width ranged from 0.10 to 0.40mm. Compared to those in standard designed implants, the maximum Von Mises stresses in cortical and cancellous bones with axially loaded implants decreased by 18.85% and 47.46%, respectively, and by 16.38% and 63.46%, respectively in buccolingually loaded implants. The maximum displacement of implant–abutment complex loaded axially and buccolingually decreased by 13.78% and 6.97%, respectively. Guan *et al.* (2011) using the finite element techniques, the stress characteristics within the mandible are evaluated during a dynamic simulation of the implant insertion process. Implantation scenarios considered are implant thread forming (S1), cutting (S2) and the combination of forming and cutting (S3). Ultimately, the out come of this study will provide an improved understanding of the failure Mechanism consequential to the stress distribution characteristics in the mandible during the Implantation process. However, Okumura *et al.* (2010) made a study of the effect of maxillary cortical bone thickness, implant design and diameter on stress around implants. Wang *et al*. (2009) created an accurately dimensioned finite element model with spiral threads and threaded bores included in the implant complex, positioned in a bone model, and to determine the magnitude and distribution of the force transformation/stress/strain patterns developed in the modeled implant system and bone and, thus, provide the foundational data for the study of the dynamic loading of dental implants prior to any external loading. FEA of Wirley Goncalves Assunção *et al.* (2011) led to the evaluation the effect of different levels of unilateral angular misfit on preload maintenance of retention screws of single implant-supported prostheses submitted to mechanical cycling.

In this study, we used a finite element method to evaluate the maximum Von Mises stresses within the mandible in the dental prosthesis during a static and dynamic loading using 3D and to determine the magnitude and distribution of the equivalent stress in the different components of the complex dental structure. The level of the stress is analysed in the proximal, median and distal zone of the bone - implant interface. The success or failure of an implant is determined by the manner that the stresses at the bone - implant interface transfer to the bone.

2. Three-dimensional representation of bone-implant models

A 3-D model of a mandible section of bone was used in this study. Data acquisition for bone dimensions are based on computed tomography scanned images. A bone block, 23.5 mm high and 15.8 mm wide, representing the section of the mandible. It consisted of a spongy center surrounded by 2 mm of cortical bone.

The geometry of the solid implant is presented in form of cylinder screw of length 8 mm and diameter 4.8 mm. Abutment of 5 mm long of conical form is adjusted to the implant.

The crown and framework model were designed in Rhinoceros 3D and SolidWorks 3D with 5° inclination in bucco-lingual direction.

The complete model that consists of crown, framework, abutment, implant, cortical and

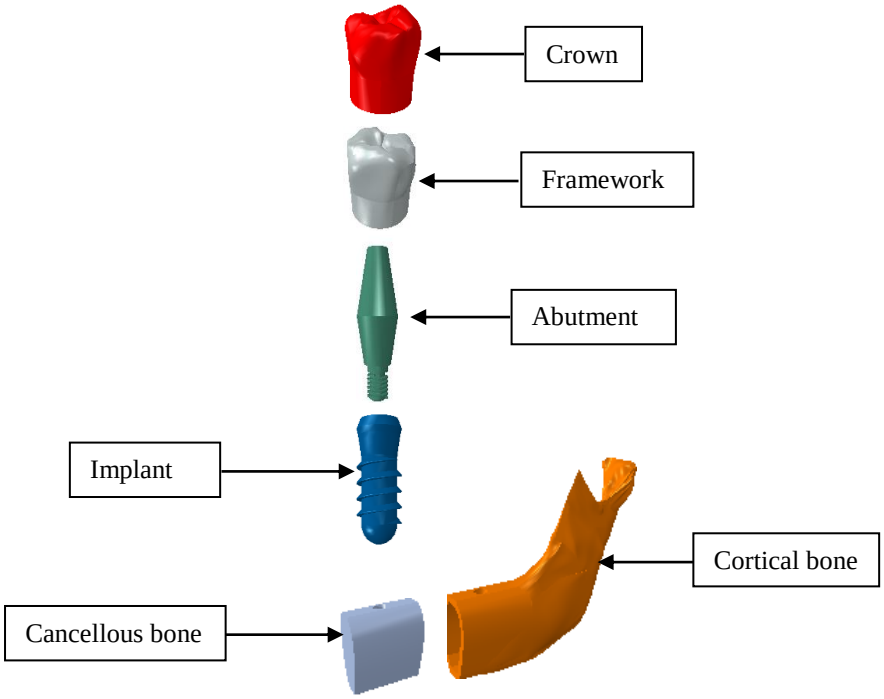

Fig. 1 Components of dental prosthesis system

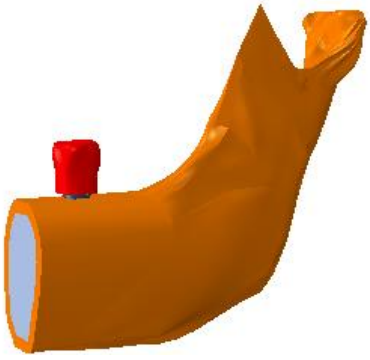

Fig. 2 Complete model of the structure

cancellous bone (Fig. 1),were assembled using SolidWorks 2008 software, and then exported to ABAQUS program.

2.1 Modelling contact

Interaction between the bone and implant during dynamic simulation of the implantation process is complex and requires definition of contact conditions. In the present study, contact is defined in ABAQUS (2007) using surface-to-surface discretisation because it provides more accurate stress and pressure results than node-to-surface discretisation.

Table 1 Mechanical properties of materials used in the study (Kayabasi *et al.* 2006)

Material		Young's modulus (GPa)	Poisson ratio (υ)	Yield strength (MPa)
Ti-6Al-4V		110	0.32	800
Cobalt-chrome alloy		220	0.30	720
Feldsphatic porcelain		61.2	0.19	500
Bone	Cortical	$Ex=Ey$=11.5 GPa, Ez=17 GPa, Gxy=3.6 GPa, $Gxz=Gyz$=3.3 GPa	vxy=0.51 $vxz=vyz$=0.31	130
	Cancellous	2.13	0.3	130

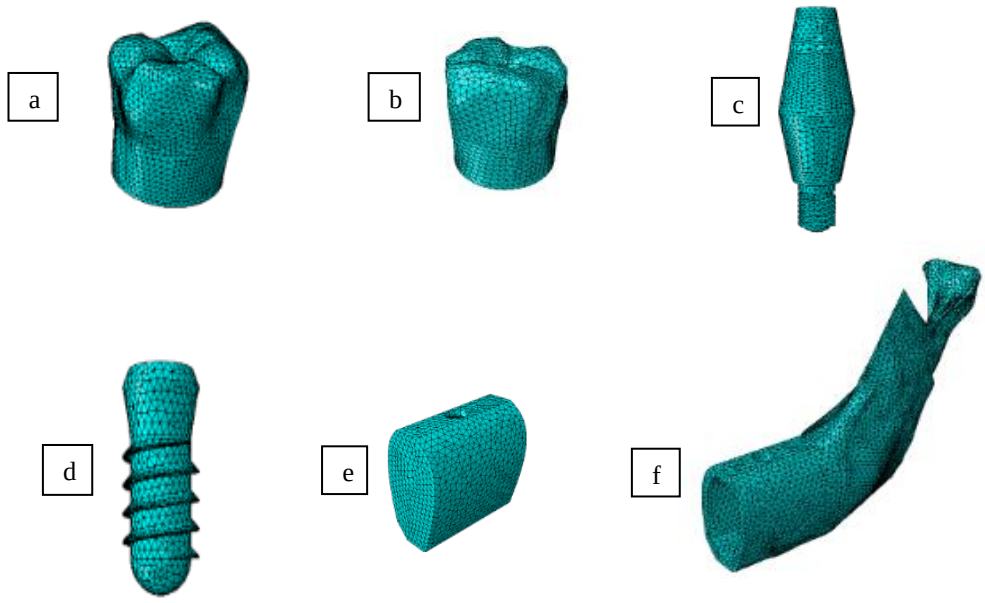

Fig. 3 Finite element models of Crown (a), Metal Framework (b), Abutment(c), Implant (d) and bone (cancellous (e), cortical (f)) respectively

ABAQUS enforces conditional constraints on each surface to simulate contact conditions. In addition, the contact interaction properties are also required to be defined for the contact pair. The bone-implant interfaces were assumed to be 100% osseointegrated (Fig. 2).

2.2 Material and methods

Ti-6Al-4V for implant and abutment, cobalt–chromium alloy for metal framework, feldsphatic porcelain for crown are used in the finite element analyses. Behaviors of these materials are represented with linear isotropic material models. Mechanical properties of materials used in this study are shown in Table 1. The cortical bone is represented with transversely isotropic material model and the cancellous bone is modeled with linear isotropic.

2.3 Finite element model

Models were meshed with tetrahedron elements. The finite element models as shown in Figs. 3-4.

Fig. 4 Finite element model of the structure

Table 2 Number of elements and nodes used in finite element model

		Number of nodes	Number of elements
Framework		48152	23786
Crown		48917	24316
Abutment		53940	26945
Implant		31972	15931
Bone	Cortical	80491	40162
	Cancellous	114357	56981

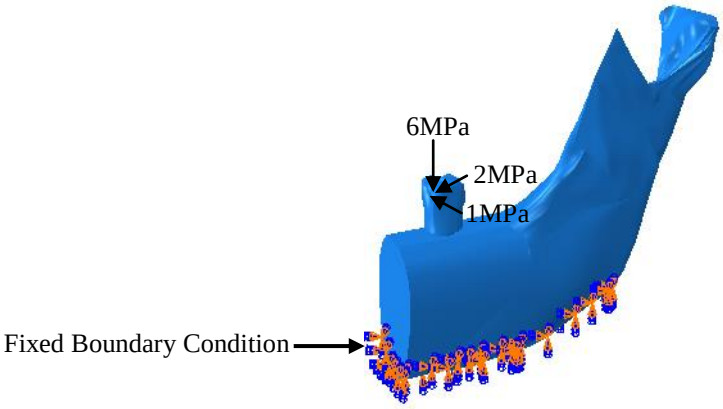

Fig. 5 Applied loads and Boundary conditions

The number of elements and nodes used in this study are given in Table II.

3. Loading conditions

In three dimensions, three dynamic loads of 6 MPa, 2 MPa and 1 MPa were separately applied

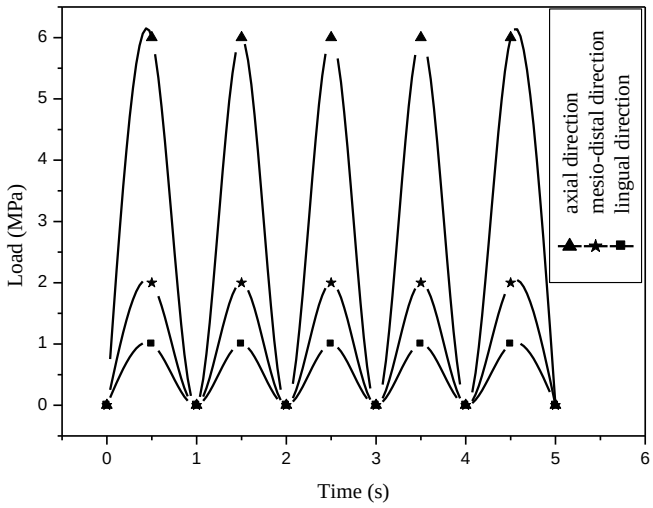

Fig. 6 Dynamic loading in 5 sec

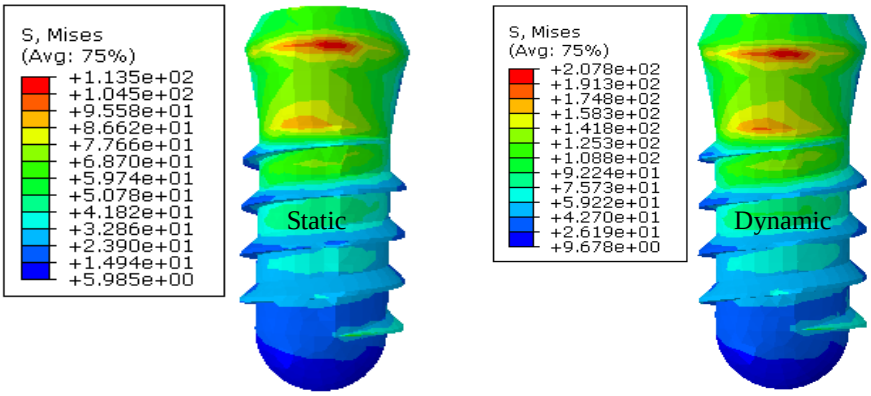

Fig. 7 Equivalent stress distribution in the implant in static and dynamic loading

in the in a lingual, an axial, and a mesiodistal direction, respectively to the center of the crown (Fig. 5). For dynamic analysis, time dependent masticatory load is applied. Time history of the dynamic load components for 5 s is demonstrated in Fig. 6. Stress levels were calculated using von Mises stresses values (Timoshenko and Young 1968). Von Mises stresses are most commonly reported in FEA studies to summarize the overall stress state at a point.

The extent of these forces depends on the applied torque as well as on the stiffness and the Friction between the involved materials (Jabbari *et al.* 2008a, b) and may significantly influence the longevity of the implant - abutment assembly (Quek *et al.* 2008). After placement of the implant, the abutment screw was tightened to the suggested torque. The abutments were attached to the implant with a tightening torque of 3500 N.mm by Kayabasi *et al.* (2006). The insertion torque generated a 3500 N.mm at the implant - bone interface.

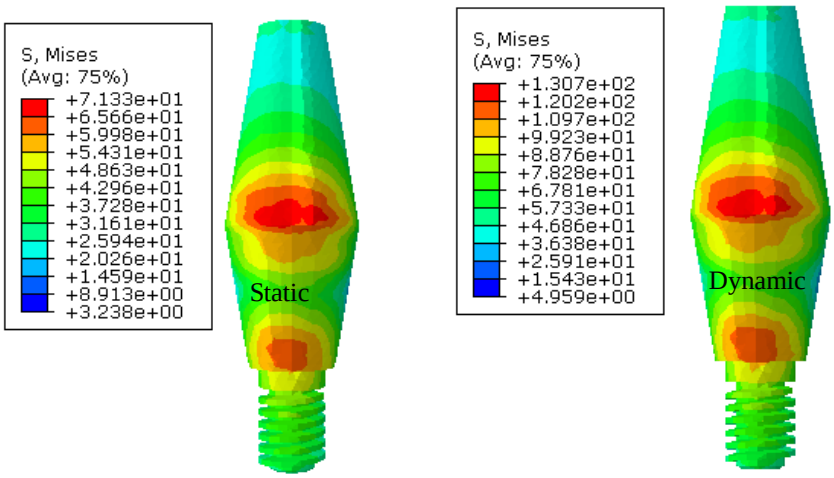

Fig. 8 Equivalent stress distribution in the abutment in static and dynamic loading

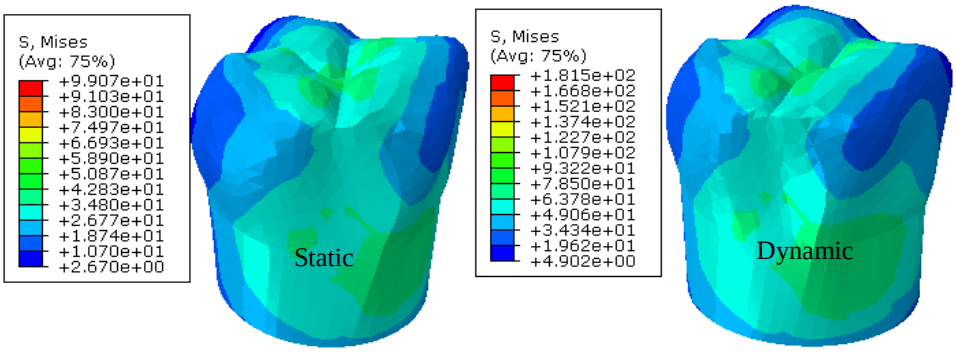

Fig. 9 Equivalent stress distribution in the metal Framework in static and dynamic loading

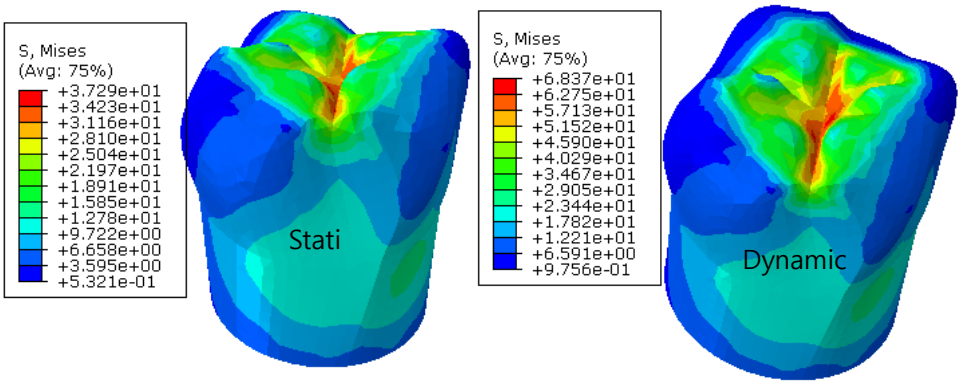

Fig. 10 Equivalent stress distribution in the crown in static and dynamic loading

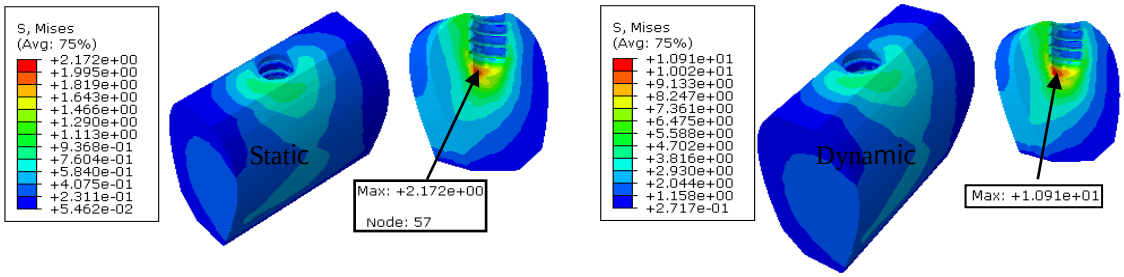

Fig. 11 Equivalent stress distribution in the cancellous bone in static and dynamic loading

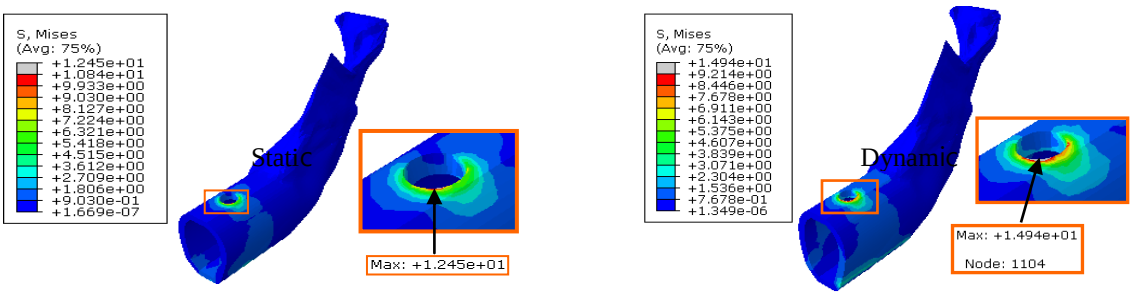

Fig. 12 Equivalent stress distribution in the cortical bone in static and dynamic loading

4. Results

In first step of this study, the mechanical responses of the prosthesis components under combined static and dynamic load are displayed in Fig. 7, Fig. 8, Fig. 9, Fig. 10, Fig. 11 and Fig. 12

4.1 Von Mises stress distribution

4.1.1 Implant

Fig. 7 represent the Von Mises stress distribution in the implant in static and dynamic loading. Maximum stresses were located on the upper part of implant at the neck for both loading conditions. The intensities of the stress in the other zone under this loading are slightly weak. Maximum Von Mises stresses for the implant in static and dynamic loading were 113.5 and 207.8 MPa, respectively. Maximum stress values at the implant body of two loading conditions were lower than the yield strength (yield point for CP titanium, 462 MPa).

4.1.2 Abutment

The stress distribution in this component was analyzed under the effect of static and dynamic loading. These stresses are strongly concentrated at the interface between the abutment and the implant at the connection between the shank and first thread of the abutment as it is shown in Fig. 8. The highest Von Mises stress value was found for the abutment in dynamic loading. For all two loading conditions, maximum Von Mises stress values in the abutment did not reach the yield strength.

4.1.3 Metal framework

Fig. 9 represent the stress distribution in the metal framework in static and dynamic loading. The maximum stresses are concentrated at the interface between the framework and abutment. In the mesial side of the framework, there is the region of strong stress concentration. In the others regions of these component, the stresses are almost uniformly distributed and their intensities remain low. Maximum Von Mises stresses for the metal framework in static and dynamic loading were 99.07 and 181.5 MPa, respectively. Maximum stress values at the metal framework of two loading conditions were lower than the yield stress (yield point for Co-Cr alloy, 720 MPa).

4.1.4 Crown

The stress distribution in this element was analyzed under the effect of static and dynamic loadings as shown in Fig. 10. In the upper part of the crown, the stress intensity is very important where the dynamic loading is applied. However, the lowest stress value was calculated in static loading. For all two loading conditions, maximum Von Mises stress values in the crown did not reach the yield strength.

4.1.5 Cortical bone

The stress distribution in this element was analyzed under the effect of static and dynamic loadings (Fig. 12). The highest von Mises stress was located on the upper part of the cortical bone surrounding the implant neck. The highest Von Mises stress value was found for dynamic loading. However, the lowest stress value was calculated for the cortical bone in the static loading. For the static loading, the maximum stress value for the cortical bone was 18% of the yield stress (yield point for cortical bone, 69 MPa). Maximum stresses for the cortical bone of dynamic loading reached 21% of the yield stress. For all two loading conditions, maximum Von Mises stress values in the cortical bone did not reach the yield strength.

4.1.6 Cancellous bone

Fig. 11 represent the stress distribution in the cancellous bone in static and dynamic loading.

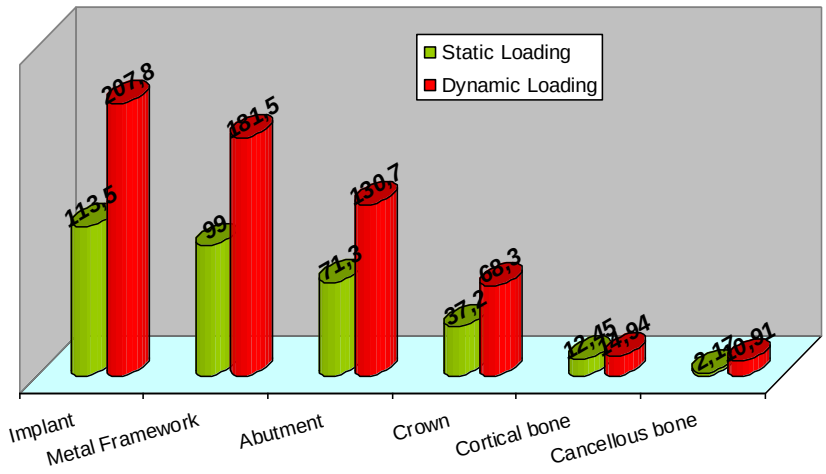

Fig. 13 Maximum comparison histogram of the Von Mises stresses between static and dynamic loading (MPa)

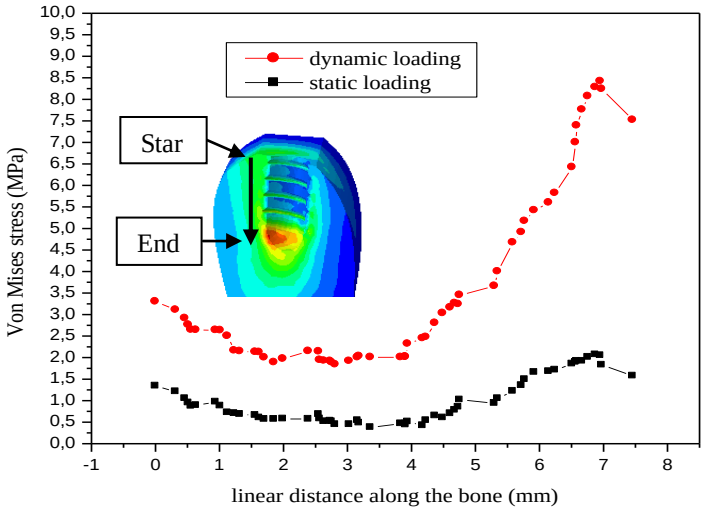

Fig. 14 Variation of the equivalent stress along the bone

The intensities of the stress in the cancellous bone under this loading are slightly weak. The highest Von Mises stress was observed at the implant bottom.

Fig. 13 represent the histograms of comparison of maximum equivalent stress that occurred at the dental prosthesis component under static and dynamic loading.

4.2 Stress distribution along the interface bone-implant

In second step of this study, the distribution of the equivalent stress in the cancellous bone at the contact of the implant is analyzed.

We analyzed the variation of the equivalent stress along the bone according to nature of loading. Fig. 14 illustrates the level and distribution of the stress induced in this living element under the effect of the static and dynamic loading.

The analysis of this figure shows, that independently of the type of loading applied to the dental structure, the equivalent stress decrease then increases sharply to the upper part of the bone to the lower part, at the contact with the implant.

This behavior shows that this element is slightly requested in its central part. We note however, the dynamic loading induced in this living tissue the stress more intense than those resulting from the static loading. These results have us conduit to analyze the variation of the Von Mises stress induced in the bone along the helicoids in its three zones (proximal, median and distal), these stresses were evaluated in this component of the dental structure in its parts upper, central and distal according to the nature of the loading (static and dynamic).

4.2.1 Variation of the equivalent stress in the proximal, Median and Distal zones of the cancellous bone under the effect of static and dynamic loading

For a better study of the stress distribution in the bone we analyzed the intensity of the Von Mises stress in three zones of this component. Indeed, these stresses are defined at the upper part, the center and the median part of the bone following the zones (proximal, median and distal).

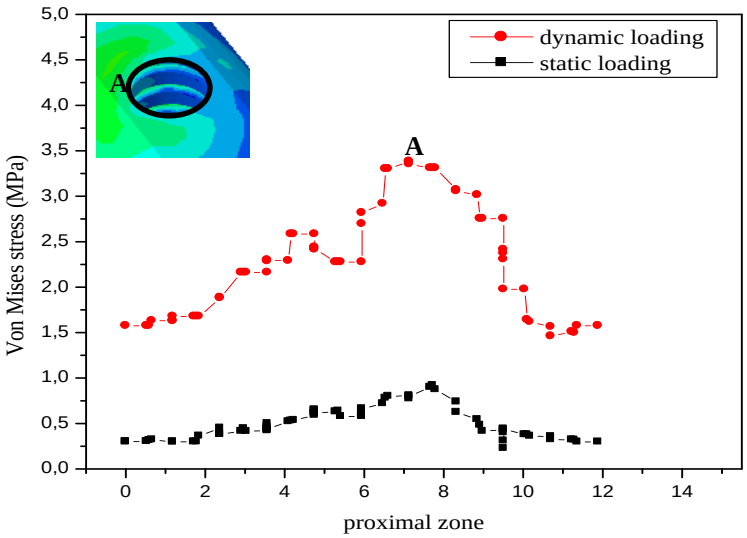

Fig. 15 Variation of the equivalent stress in the proximal zone of the bone under the effect of a static and dynamic loading

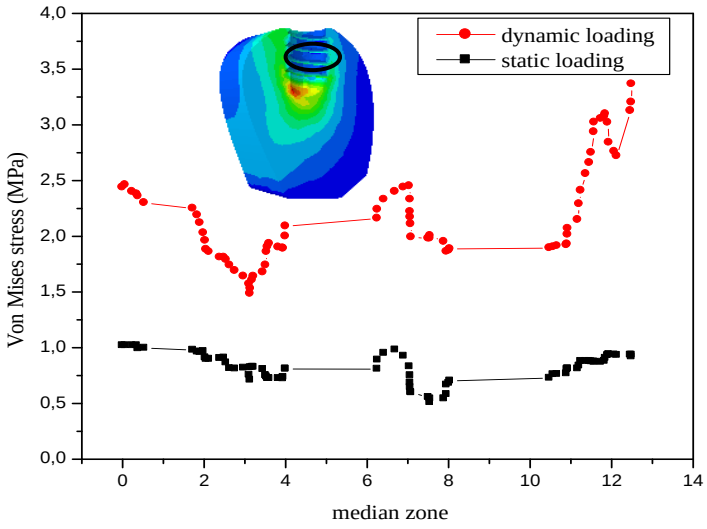

Fig. 16 Variation of the equivalent stress in the median zone of the bone under the effect of a static and dynamic loading

Fig. 15 illustrates the variation of the Von Mises stress in the proximal zone of the bone along the helicoid under the effect of the static and dynamic loading. This figure shows that this stress increase, reached its maximum level then decrease for towards its initial level. The strongest

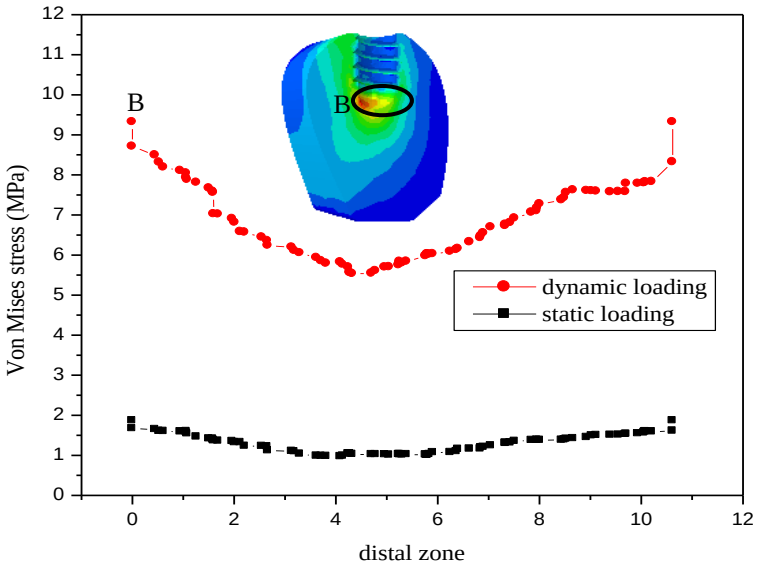

Fig. 17 Variation of the equivalent stress in the distal zone of the bone under the effect of a static and dynamic loading

stresses are observed on the area of high contact with the implant. The intensity of the equivalent stress induced in this zone of the bone under the dynamic loading is more important than that generated in the static loading.

The Fig. 16 represents the variation of the Von Mises stress in the median zone of the bone under the effect of static and dynamic loading. Compared to the stress induced in the proximal zone, the lowest stress value is observed. The strongest stresses are located on the part in contact with the implant. These stresses are the more intense when the dental prosthesis is subjected to a dynamic loading.

The variation of the equivalent stress of Von Mises in the distal zone of the bone along the helicoid of static and dynamic loading is illustrated in Fig. 17. This intensity of the stress decrease then increases along this helicoid to reach its optimum. The highest stresses level of the equivalent stress is observed in the zone of contact implant-bone. In this zone (distal) or the bone is more strongly requested. The dynamic loading generates in this part of the bone much more important equivalent stresses.

5. Conclusions

According to the results and within the limitations of the present study, it was concluded that:

• The dynamic loading induced in the dental prosthesis the equivalent stress more important than those resulting from the static loading.

• The equivalent stress of Von Mises in the elements (crown, framework, abutment, implant, bone) of the dental prosthesis are not distributed in a homogeneous, the zones of contacts element-element are the area of stress concentration.

• Compared to the static efforts, the dynamic loadings induce stress of Von Mises in the

components of the dental structure approximately doubly more intense.

• The bone the weakest element of the dental structure, is strongly requested in its bottom part, part of contact with the implant. Its median part is most slightly solicited.

• The Von Mises equivalent stresses induced in the three zones (proximal, median and distal) of the bone along the helicoids are not distributed uniformly. Their maximum intensity is reached in the part in strong contact with the implant. The strongest stresses are located on the distal zone of the bone.

References

ABAQUS (2007), http: *www.simulia.com*, accessed 5 February.

Al Jabbari, Y.S., Fournelle, R., Ziebert, G., Toth, J. and Iacopino, A.M. (2008a), "Mechanical Behavior andfailure analysis of prosthetic retaining screws after long-term use invivo. Part1: characterization of adhesive wear and structure of retaining screws", *J. Prosthodont*, **17**, 80-168.

Al Jabbari, Y.S., Fournelle, R., Ziebert, G., Toth, J. and Iacopino, A.M. (2008b), "Mechanical behavior and failure analysis of prosthetic retaining screws after long-term use invivo. Part 2: metallurgical and micro hardness analysis", *J. Prosthodont*, **17**, 91-181.

Ao, J., Li, T., Liu, Y., Ding, Y., Wu, G., Hu, K. and Kong, L. (2010), "Optimal design of thread height and width on an immediately loaded Cylinder implant: a finite element analysis", *Comput. Bio. Med.*, **40**, 681-686.

Assunção, W.G., Barão, V.A.R., Delben, J.A., Gomes, É.A. and Garcia, I.R. (2011), "Effect of unilateral misfit on preload of retention screws of implant supported prostheses submitted to mechanical cycling", *J. Prosthod. Res.*, **55**, 12-18.

Block, M.S., Kent, J.N. and Guerra, L. (1997), "Implants in dentistry: essentials of endosseous implants for maxillofacial reconstruction", *Biomechanics of Dental Implants*, **63-71**, Philadelphia, USA.

Dittmer, M.P., Dittmer, S., Borchers, L., Kohorst, P. and Stiesch, M. (2011), "Influence of the interface design on the yield force of the implant-abutment Complex before and after cyclic mechanical loading", *J. Prosthod. Res.*, **8**, 19-24.

Geng, J., Tan, K. and Liu, G. (2001), "Application of finite element analysis in implant dentistry", *J. Prosthet Dent*, **85**(6), 585-598.

Guan, H., van Staden, R.C., Johnson, N.W. and Loo, Y.C. (2011), "Dynamic modelling and simulation of dental implant insertion process-A finite element study", *Finite Elem. Anal. Des.*, **47**, 886-897.

Hoyer, S.A., Stanford, C.M., Buranadham, S., Fridrich, T., Wagner, J. and Gratton, D. (2001), "Dynamic fatigue properties of the dental implant-abutment interface: Joint opening in wide-diameter versus standard-diameter hex-type implants", *J. Prosthetic Dent.*, **85**, 599-607.

Kayabasi, O., Yuzbasioglu, E. and Erzincanli, F. (2006), "Static, dynamic and fatigue behaviours of dental implant using finite element method", *Adv Eng Softw*, **37**, 58-649.

Koca, O.L., Eskitascioglu, G. and Usumez, A. (2005), "Three dimensional finite element analysis of function al stresses in different bone locations produced by implants placed in the maxillary posterior region of the sinus floor", *Journal of Prosthet Dent*, **93**, 38-44.

Okumura, N., Stegaroiu, R., Kitamura, E., Kurokawa, K. and Nomura, S. (2010), "Influence of maxillary cortical bone thickness, implant design and implant diameter on stress around implants: a three-dimensional finite element analysis", *J. Prosthod. Res.*, **54**, 133-142.

Quek, H.C., Tan, K.B. and Nicholls, J.I. (2008), "Load fatigue performance of four implant-abutment interface designs: effect of torque level and implant system", *J. Oral Maxillof. Implants*, **23**, 62-253.

Rached, R.N., de Souza, E.M., Dyer, S.R. and Ferracane, J.L. (2011), "Dynamic and static strength of an implant-supported overdenture model reinforced with metal and non-metal strengtheners", *J. Prosthetic Dent.*, **106**, 297-304

Timoshenko, S. and Young, D.H. (1968), *Elements of Strength of Materials*, 5th Edition, Florence, Wadsworth.

Van Osterwyck, H., Duyck, J., Vander, S., Vander, P.G., Decoomans, M., Lieven, S., Puers, R. and Naert, L. (1998), "The influence of bone mechanical properties and implant fixation upon bone loading around oral implants", *Clinic Oral Implants Res.*, **9**(6), 407-412.

Wang, R.F., Kang, B., Lang, L.A. and Razzoog, M.E. (2009), "The dynamic natures of implant loading", *J. Prosthetic Dent.*, **101**, 359-371.

Zarb, G.A. and Schmitt, A. (1990), "The longitudinal clinical effectiveness of osseointegrated implants", *J. Prosthet Dent*, **64**, 94-185.

Zinser, M., Neugebauer, J., Mischkowski, R.A., Karapedian, V.E., Kübler, A. and Zöller, J.E. (2004), "Comparison of static and dynamic navigation systems for insertion of dental implants", *Int. Congress Series*, **1268**, 1378, June.

CC